Supplementary Information for "Orbital-selective time-domain signature of nematicity dynamics in the charge-density-wave phase of $La_{1.65}Eu_{0.2}Sr_{0.15}CuO_4$"

Martin Bluschke,[1,2,†,*] Naman K. Gupta,[3,†] Hoyoung Jang,[4,5] Ali. A. Husain,[1,2] Byungjune Lee,[6,7] Minjune Kim,[1,2] MengXing Na,[1,2] Brandon Dos Remedios,[1,2] Steef Smit,[1,2] Peter Moen,[1,2] Sang-Youn Park,[4] Minseok Kim,[4] Dogeun Jang,[4] Hyeongi Choi,[4] Ronny Sutarto,[8] Alexander H. Reid,[9] Georgi L. Dakovski,[9] Giacomo Coslovich,[9] Quynh L. Nguyen,[9,10] Nicolas G. Burdet,[9,11] Ming-Fu Lin,[9] Alexandre Revcolevschi,[12] Jae-Hoon Park,[6,7] Jochen Geck,[13,14] Joshua J. Turner,[9,11] Andrea Damascelli,[1,2,*] and David G. Hawthorn[3,*]

[1] *Quantum Matter Institute, University of British Columbia; Vancouver, British Columbia V6T 1Z4, Canada.*

[2] *Department of Physics & Astronomy, University of British Columbia; Vancouver, British Columbia V6T 1Z1, Canada.*

[3] *Department of Physics & Astronomy, University of Waterloo; Waterloo, Ontario N2L 3G1, Canada.*

[4] *PAL-XFEL, Pohang Accelerator Laboratory; Pohang, Gyeongbuk 37673, Republic of Korea.*

[5] *Photon Science Center, Pohang University of Science and Technology; Pohang, Gyeongbuk 37673, Republic of Korea.*

[6] *Max Planck POSTECH/Korea Research Initiative, Center for Complex Phase Materials; Pohang 37673, Republic of Korea.*

[7] *Department of Physics, Pohang University of Science and Technology; Pohang 37673, Republic of Korea.*

[8] *Canadian Light Source; Saskatoon, Saskatchewan S7N 2V3, Canada.*

[9] *Linac Coherent Light Source, SLAC National Accelerator Laboratory; Menlo Park, California 94025, USA.*

[10] *Stanford PULSE Institute, Stanford University and SLAC National Accelerator Laboratory; Menlo Park, California 94025, USA.*

[11] *Stanford Institute for Materials and Energy Sciences, SLAC National Accelerator Laboratory and Stanford University; Menlo Park, California 94025, USA.*

[12] *Institut de Chimie Moléculaire et des Matériaux d'Orsay, Université Paris-Saclay; CNRS, UMR 8182, 91405 Orsay, France.*

[13] *Institute of Solid State and Materials Physics, TU Dresden; 01069 Dresden, Germany.*

[14] *Würzburg-Dresden Cluster of Excellence ct.qmat, Technische Universität Dresden; 01062 Dresden, Germany.*

† These authors contributed equally to this work.

* Corresponding authors:

martin.bluschke@ubc.ca (M.B.);

damascelli@physics.ubc.ca (A.D.);

david.hawthorn@uwaterloo.ca (D.G.H.)

Characterization of Q=(001) equilibrium temperature dependence.

The $La_{1.8-x}Eu_{0.2}Sr_xCuO_4$ single crystal investigated in this study is the same sample investigated in the context of Ref.[1], where the equilibrium temperature dependence of the Q =(001) reflection at the Cu L_3, the planar O K and the apical O K resonances was measured. These data are reproduced in Fig. S1(a), as well as in Fig. 1(b) of the main manuscript. In order to exclude sample aging effects and to verify the stability of the doping level, we measured the equilibrium temperature dependence of the (001) reflection at both the planar and apical O K resonances at the REIXS beamline of the Canadian Light Source (CLS), before performing the pump-probe measurements at the Pohang Accelerator Laboratory x-ray free electron laser (PAL-XFEL). These data are presented in Fig. S1(b). The temperature dependent (001) intensity at the apical O K resonance verifies the integrity of the crystal structure and the expected low-temperature tetragonal (LTT) phase. The temperature dependence at the planar O K resonance can be used to infer T_{CDW} and is thus an approximate measure of the doping level, which appears to have remained stable at $x = 0.15$ since the measurements presented in Ref.[1].

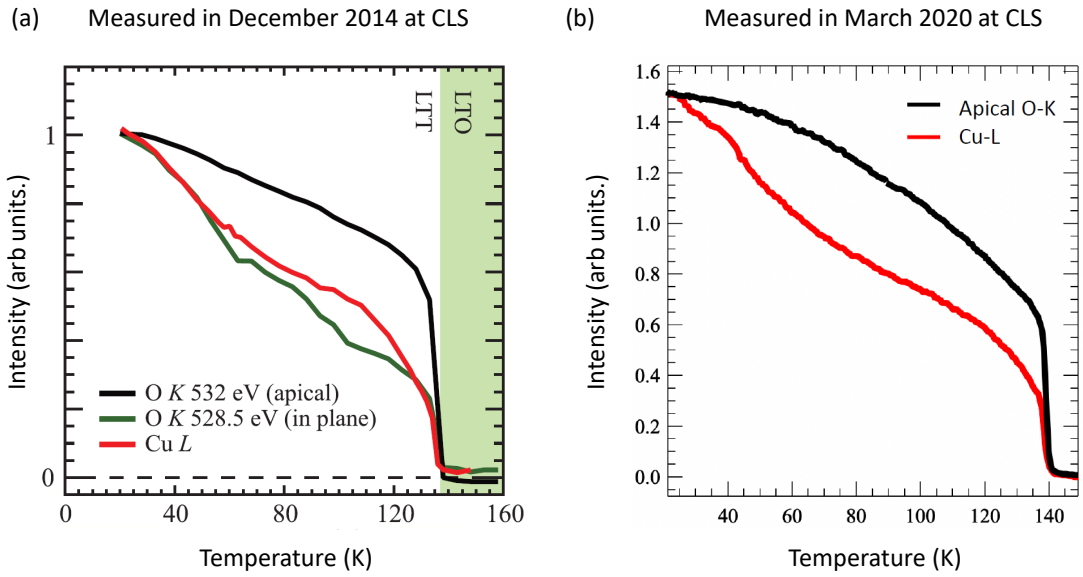

FIG. 1. **Q=(001) equilibrium temperature dependence.** (a) Comparison of the temperature dependent Q=(001) intensity measured at the apical O K, the planar O K, and the Cu L_3 resonances. These data were collected in December 2014 in the context of Ref.[1]. (b) Comparison of the temperature dependent Q=(001) intensity measured at the apical O K and the Cu L_3 resonances. These data were collected in March 2020 in preparation for the non-equilibrium measurements presented in the main manuscript.

High-fluence pump-induced dynamics at Q=(001)

In Fig. S2(a) we plot the low temperature (20 K) pump-induced dynamics at the apical and planar O K resonances for a series of pump fluences. The apical O data demonstrates the time-resolved suppression of the LTT distortion

and is identical to the data plotted in Fig. 2 of the main manucript, but shown for a shorter range of time delays. At the planar O K resonance the low-fluence signal is dominated by nematicity dyanamics, which is the focus regime of the main manuscript, whereas at higher fluences nematicity dynamics are observed together with the suppression of the LTT distortion. These data are presented in Fig. S2(b). In Fig. S3, x-ray absorption spectroscopy (XAS) at the O K edge is shown for reference, indicating the features corresponding to the planar and apical O resonances.

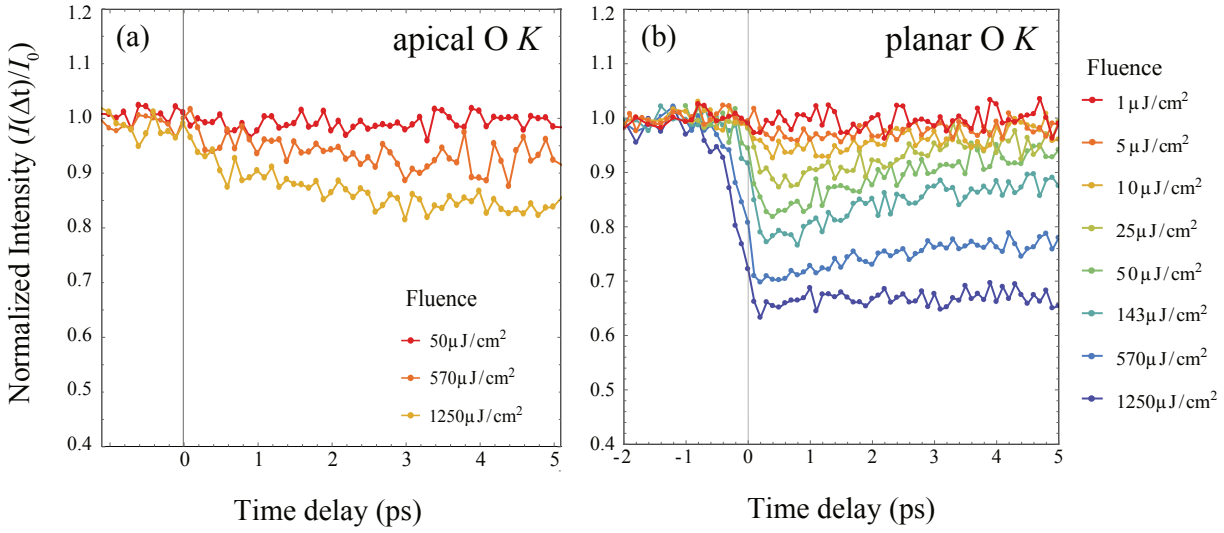

FIG. 2. **High fluence dynamics at O K resonances.** (a) Q=(001) pump-induced dynamics measured at the apical oxygen K resonance at 20 K. (b) Q=(001) pump-induced dynamics measured at the planar oxygen K resonance at 20 K.

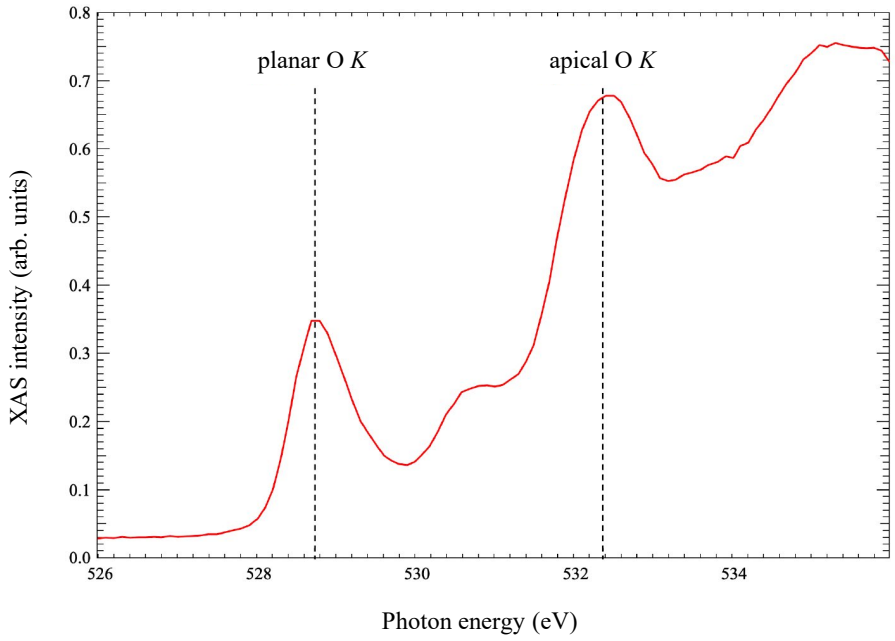

FIG. 3. **O K XAS.** Equilibrium XAS measured across the O K edge at 20 K in the total electron yield mode.

Charge density wave detection at Q_{CDW}

In Fig. S4 an angular (theta) scan through Q_{CDW} at 20 K is plotted both in equilibrium, as well as out-of-equilibrium at 0.5 ps following excitation with a 1350 μJ/cm^2 pump pulse. These scans were collected using an avalanche photodiode with a 2 mm aperature, at a distance of 90 mm from the sample. The Q_{CDW} reflection was observed at the Cu L_3 resonance (931.7 eV) using a detector angle (Two theta) of 164° corresponding to an out-of-plane momentum transfer of $L = 1.74$. This geometry was chosen based on previous experience to minimize the variation of the background intensity as a function of the incidence angle theta. The component of the momentum transfer parallel to the CuO_2 planes was aligned with the Cu-O-Cu bond direction by locating the equilibrium (103) Bragg peak at the REIXS enstation of the CLS and then transfering the sample in this orientation to the RSXS endstation at the PAL-XFEL.

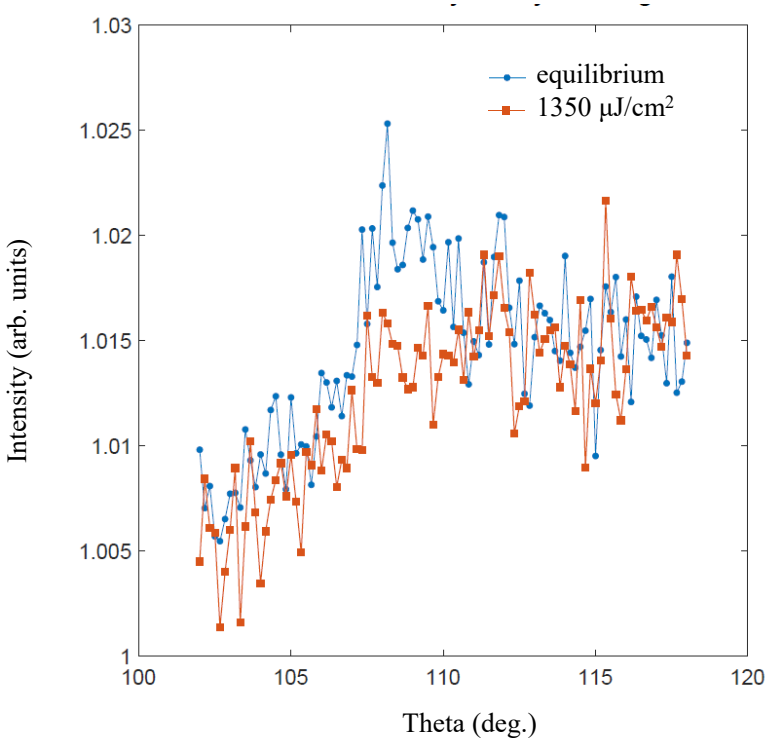

FIG. 4. **Charge scattering at Q_{CDW}** The CDW scattering intensity is measured in and out of equilibrium as a function of incidence angle (theta) in a laser on/off scan. The laser on data was collected at a time delay of +0.5 ps following the pump excitation.

Time trace fitting

The time-resolved resonant x-ray scattering (tr-RXS) intensities presented in Fig. 3 of the main manuscript are modelled using an approach in which the dynamics are divided into an electronic (nematic or CDW) and a lattice

contribution. The electronic contribution experiences a time-resolution limited suppression (step function at $\Delta t = 0$), and an exponential recovery with time constant τ_1.

$$\Delta I_{electronic}(\Delta t) = \begin{cases} 0 & \Delta t < 0 \\ -a_1 \exp^{-\Delta t/\tau_1} & \Delta t \geq 0 \end{cases}$$

In contrast, the dynamic response of the lattice, e.g. the LTT distortion, is not immediately activated by the incident pump photons but onsets exponentially with time constant τ_2 as energy is transferred from the hot electronic system to the lattice.

$$\Delta I_{lattice}(\Delta t) = \begin{cases} 0 & \Delta t < 0 \\ a_2(\exp^{-\Delta t/\tau_2} - 1) & \Delta t \geq 0 \end{cases}$$

In order to reduce the number of fitting parameters, $\tau_2 = 1.6$ ps is determined from fitting to the $\Delta I_{lattice}$ model to the dynamics measured at the Apical O K resonance (Fig. 1(E) of main manuscript). τ_2 is then held constant when fitting the electronic dynamics measured at Cu L_3 resonance. Examples of the time-dependent dynamics of the electronic and lattice models are shown in Fig. S5(a). The quantity being modelled is the time-dependent scattering intensity normalized to the equilibrium scattering intensity ($I(\Delta t)/I_0$). The full model, shown in Fig. S5(b) is achieved by summing the equilibrium scattering I_0 with the functions representing the time dependent suppression of scattering intensity with electronic and lattice like dynamics. The entire sum is normalized to I_0 and then convolved with a gaussian of width 110 fs to account for the finite temporal resolution of the experiment.

$$I(\Delta t)/I_0 = (I_0 + \Delta I_{electronic} + \Delta I_{lattice})/I_0 .$$

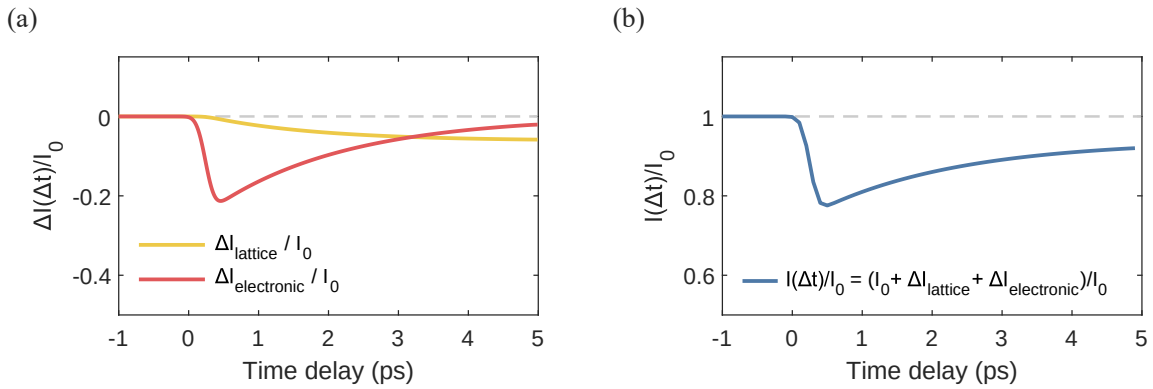

FIG. 5. **Modelling of electronic and lattice dynamics.** (a) The model for time-dependent suppression of scattering intensity associated with electronic order, i.e. CDW or nematic, is compared with the model for lattice-like dynamics. (b) The full model for time dependent scattering observed at the Cu L_3 resonance comprises both electronic and a lattice like dynamics.

When fitting the data presented in Fig. 3 of the main manuscript, an alternate model for the electronic dynamics was considered, comprising two exponential recovery terms.

$$\Delta I_{electronic}(\Delta t) = \begin{cases} 0 & \Delta t < 0 \\ -a_0 \exp^{-\Delta t/\tau_0} - a_1 \exp^{-\Delta t/\tau_1} & \Delta t \geq 0 \end{cases}$$

Fits using 1 versus 2 exponentials for the electronic recovery dynamics are compared in Fig. S 6, along with their residuals. In the case of the $Q = (0\ 0\ 1)$ scattering, the fit with 2 exponential recovery terms returns twice the same time constant, confirming that the recovery is well described by a single exponential. For the Q_{CDW} scattering, the fit with 2 exponential recovery terms returns time constants $\tau_0 = 0.7$ ps and $\tau_1 = 4.2$ ps. For Q_{CDW}, the fits using one and two exponentials to model the recovery are essentially indistinguishable from one another.

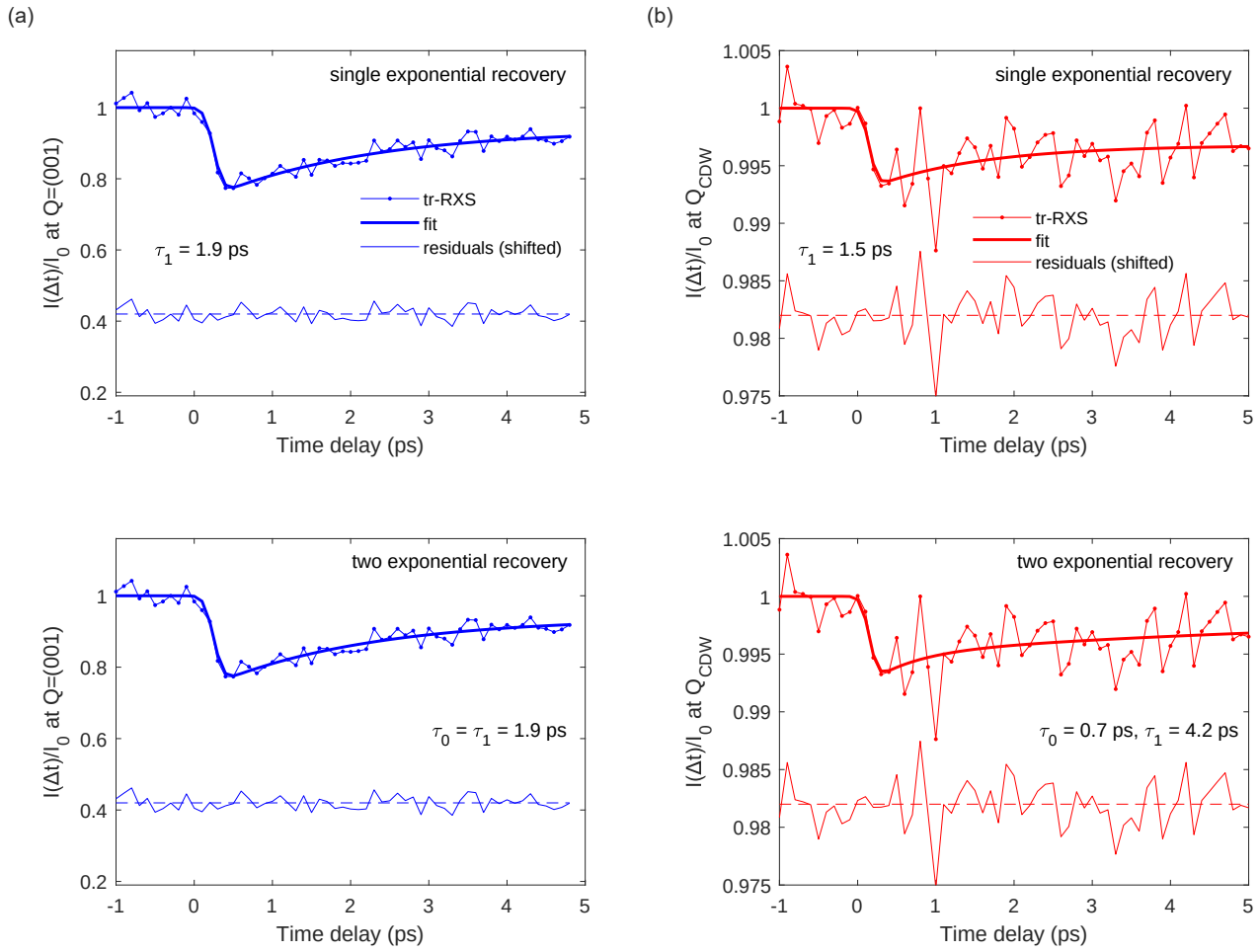

FIG. 6. **One and two exponential model for electronic recovery dynamics.** Comparison of fits to the tr-RXS data presented in Fig. 3 of the main manuscript at (a) $Q = (0\ 0\ 1)$ and (b) Q_{CDW}, using models with one and two exponential recovery terms to capture the electronic dynamics. In each case the residuals are shown, shifted to within the field of view. The two fits to $Q = (001)$ data shown in (a) are identicle to one another, whereas the fits to Q_{CDW} in (b) are distinct but almost indistinguishable.

References

1. A. J. Achkar, M. Zwiebler, C. McMahon, F. He, R. Sutarto, I. Djianto, Z. Hao, M. J. P. Gingras, M. Hücker, G. D. Gu, A. Revcolevschi, H. Zhang, Y.-J. Kim, J. Geck, and D. G. Hawthorn, Nematicity in stripe-ordered cuprates probed via resonant x-ray scattering, Science **351**, 576 (2016).